



Synthesis and characterization of binuclear [ONXO]-type amine-bis(phenolate) copper(II) complexes

Elham Safaei^{a,*}, Maryam Rasouli^a, Thomas Weyhermüller^b, Eckhard Bill^b

^a Institute for Advanced Studies in Basic Sciences (IASBS), 45195 Zanjan, Iran

^b Max-Planck Institute for Bioinorganic Chemistry, Stiftstraße 34-36, D-45470, Mülheim an der Ruhr, Germany

ARTICLE INFO

Article history:

Received 16 November 2010

Received in revised form 16 February 2011

Accepted 30 April 2011

Available online 12 May 2011

Keywords:

Magnetism

Amine bis(phenolate)

Model complexes

Phenoxy

ABSTRACT

Dimeric copper(II) complexes [Cu^{II}₂L₂] of a series of amine-bis(phenolate) ligands (H₂L) bearing different non- or weakly coordinating side-arms such as ethyl (H₂L^{Et}), *n*-butyl (H₂L^{Bu}), thiomethyl (H₂L^{SMe}) and hydroxyl (H₂L^{OH}) were synthesized. They were characterized by X-ray crystallography, UV–Vis, IR and magnetic susceptibility measurements. X-ray analysis revealed complexes in which Cu(II) centers are surrounded by three phenolate oxygen atoms, an amine nitrogen atom and thiomethyl and hydroxyl coordinating groups in Cu₂L^{SMe}₂ and Cu₂L^{OH}₂, respectively. Two phenolate bridges hold both copper atoms together to form binuclear [Cu^{II}₂L₂] complexes. To the best of our knowledge, Cu...Cu distances and Cu–O–Cu bridge angles of these complexes are the smallest values, which have been reported for phenoxo-bridged copper complexes to date. Phenolate moieties of the copper complexes can be electrochemically oxidized to phenoxy radicals. Magnetic studies show that Cu₂L^{Et}₂ and Cu₂L^{Bu}₂ are rare examples of phenolato-bridged Cu(II) dimer exhibiting ferromagnetic interaction ($J = +26.62$ and $+38.65$ cm⁻¹ respectively). In addition, an antiferromagnetic exchange with J values of -65.88 and -2.77 cm⁻¹ was found for Cu₂L^{SMe}₂ and Cu₂L^{OH}₂, respectively.

© 2011 Elsevier B.V. All rights reserved.

1. Introduction

Metalloenzymes control a wide range of functions in biological systems. These metallo-biomolecules are coordination complexes whose active sites, consist of one or more metal atoms and their coordinated ligands. The metal ions in these coordination environments cooperate with each other to complete a catalytic function [1–3]. Copper is one of these metal ions frequently found at some of the enzymes' active sites composed of donors from the side-chains of amino acids such as histidine and tyrosine holding it [4–9].

The synthetic analog approach is based on the chemistry of the enzyme's active site. Recent studies provided Cu(II) complexes with tripodal aminophenol ligands involving N₃O, N₂O₂ and NO₂ coordination spheres (N and O represent nitrogen and oxygen donor molecules such as pyridine and phenol) as synthetic analogs of tyrosine and histidine moieties of amino acids [10–20]. Significant efforts have been made to provide coordination complexes as models for active sites of multi-copper enzymes [21–24]. On the other hand, magneto chemistry of these multinuclear complexes is a subject of current interest. These complexes are classified according to their metal–metal spin interaction. These interactions are termed superexchange because of the large distances involved (3–5 Å) between the metal ions [25]. In the non interacting type,

there is not any copper(II)–copper(II) spin interaction. In the strongly interacting type, relatively strong copper(II)–copper(II) spin interaction occurs. In weakly interacting systems, coupling between the electron spins of the two copper ions leads to antiferromagnetic or ferromagnetic behavior, depending on which exchange pathway dominates spin interactions.

This study aimed to investigate the effect of an additional pendant arm on the magnetic and redox properties of the resulting complexes of amine-bis(phenol) ligands (Scheme 1). We synthesized copper complexes of mentioned ligands with different side arms such as alkyl and coordinating thiomethyl and hydroxyl moieties. The coordination, magnetic and redox properties of related binuclear Cu(II) complexes of ligands H₂L are described.

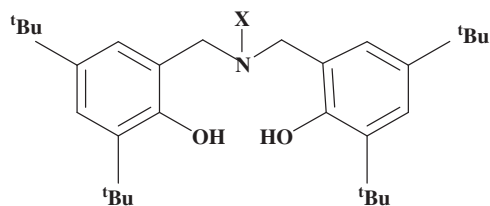
2. Experimental

2.1. Materials and physical measurements

Reagents and analytical grade materials were obtained from commercial suppliers and used without further purification, except those for electrochemical measurements. Elemental analyses (C, H, N) were performed by the Research Institute of Petroleum Industry (RIPI). Fourier transform infrared spectroscopy on KBr pellets was performed on a FT IR Bruker Vector 22 instrument. NMR measurements were done on a Bruker 250 instrument. UV–Vis absorbance digitized spectra were collected using a CARY 100 Bio

* Corresponding author. Tel.: +98 241 4153200; fax: +98 241 4153232.

E-mail address: safaei@iasbs.ac.ir (E. Safaei).



Ligand	X
H ₂ L ^{Et}	-CH ₂ CH ₃
H ₂ L ^{Bu}	-(CH ₂) ₃ CH ₃
H ₂ L ^{SMe}	-(CH ₂) ₂ SCH ₃
H ₂ L ^{OH}	-(CH ₂) ₂ OH
H ₂ L ^{OAc}	-(CH ₂) ₂ OCOCH ₃

Scheme 1. The structure of H₂L.

spectrophotometer. Magnetic susceptibility data were measured from powder samples of solid material in the temperature range of 2–290 K by using a SQUID susceptometer with a field of 1.0 T (MPMS-7, Quantum Design, calibrated with standard palladium reference sample, error < 2%). Multiple-field variable-temperature magnetization measurements were done at 1, 4, and 7 T also in the range of 2–290 K with the magnetization equidistantly sampled on a 1/T temperature scale. The experimental data were corrected for underlying diamagnetism by use of tabulated Pascal's constants [26,27] as well as for temperature-independent paramagnetism. The susceptibility and magnetization data were simulated with our own package julX for exchange coupled systems [28]. The simulations are based on the usual spin-Hamilton operator for binuclear complexes with two spins $S_1 = S_2 = 1/2$.

$$\hat{H} = -2J[\hat{S}_1 \cdot \hat{S}_2] + g\beta(\hat{S}_1 + \hat{S}_2) \cdot \vec{B} \quad (1)$$

where J is the spin coupling constant and g is the average of the electronic g matrix components (kept equal for both Cu sites). Diagonalization of the Hamiltonian was performed with the routine ZHEEV from the LAPACK Library [29] and the magnetic moments were obtained from first order numerical derivative dE/dB of the eigenvalues. The powder summations were done by using a 16-point Lebedev grid [30,31]. Intermolecular interactions were considered by using a Weiss temperature, ΘW , as perturbation of the temperature scale, $kT = k(T - \Theta W)$ for the calculation. Powder summations were done by using a 16-point Lebedev grid.

Voltammetric measurements were made with a computer controlled Auto Lab electrochemical system (ECO Chemie, Utrecht, The Netherlands) equipped with a PGSTA 30 model and driven by GPES (ECO Chemie). A glassy carbon electrode with a surface area of 0.756 cm² was used as a working electrode and a platinum wire served as the counter electrode. The reference electrode was an Ag wire as the quasi reference electrode. Ferrocene was added as an internal standard and potentials were referenced versus the ferrocenium/ferrocene couple (Fc⁺/Fc).

The X-ray data for the reported complexes were collected on a Bruker-Nonius Kappa CCD diffractometer at 100(2) K using graphite-monochromated Mo K α radiation ($\lambda = 0.71073$ Å). Final cell constants were obtained from a least-squares fit of all integrated reflections. Intensity data were corrected for Lorentz and polarization effects. The data sets were corrected for absorption (SADABS, Bruker-Nonius 2004) [32]. The structures were solved by direct

method and refined by full-matrix least-squares techniques based on F^2 (SHELXTL software package) [33].

2.2. Preparations

Ligands H₂L^{Et}, H₂L^{Bu} and H₂L^{SMe} were prepared by procedures reported in the literature [34,35]. The new ligands H₂L^{OH} and H₂L^{OAc} were synthesized by procedures reported here. As aqueous formaldehyde was one of the reagents, in some cases no added solvent was required beyond what was already present in the reagents solution.

2.2.1. Synthesis of H₂L^{Et}

A solution of 2,4-di-*tert*-butylphenol (5.0 g, 24.2 mmol), ethylamine (0.67 ml, 12.1 mmol), and 36% aqueous formaldehyde (1.62 ml, 19.4 mmol) in methanol (10 ml) was stirred and refluxed for 24 h. The mixture was cooled, filtered and the residue was washed with cold methanol, to give the product as a white powder. The product was further purified by recrystallization from dichloromethane/methanol solvent mixture (2:1). The solution remaining after the removal of the solid was left to give more product as a white powder (2.27 g, 39%). MP. 113.6 °C. ¹H NMR: (CDCl₃/250 MHz): δ 7.26 (s, 2H, C₆H₂), 6.96 (s, 2H, C₆H₂), 3.73 (s, 4H, CH₂), 2.68 (q, 2H, CH₂), 1.38 (s, 18H, C(CH₃)₃), 1.22 (s, 18H, C(CH₃)₃), 1.06 (t, $J = 7$ Hz, 3H, CH₃). IR (KBr): $\nu = 3240, 2953, 2872, 2860, 1460, 1330, 1300, 1220, 860$ cm⁻¹.

A synthesis of the ligand in aqueous media or under methanol-free condition was tested (2.33 g, 40%).

2.2.2. Synthesis of H₂L^{Bu}

A solution of 2,4-di-*tert*-butylphenol (5.0 g, 24.2 mmol), butylamine (1.2 ml, 12.1 mmol) and 36% aqueous formaldehyde (4.0 ml, 48.0 mmol) in 10 ml of methanol was stirred and refluxed for 24 h. After cooling the mixture in the freezer overnight, the solvent was removed. The residue was washed repeatedly with little amounts of cold methanol to give the product as a white powder (3.89 g, 63.2%). The product was further purified by recrystallization from dichloromethane/methanol solvent mixture (2:1). MP 102.6 °C. ¹H NMR: (CDCl₃/250 MHz): δ 7.24 (s, 2H, C₆H₂), 6.94 (s, 2H, C₆H₂), 3.70 (s, 4H, CH₂), 2.55 (t, $J = 7$ Hz, 2H, CH₂), 1.60 (m, 4H, CH₂), 1.36 (s, 18H, C(CH₃)₃), 1.11 (s, 18H, C(CH₃)₃), 0.852 (t, $J = 7.75$ Hz, 3H, CH₃). IR (KBr): $\nu = 3240, 2960, 2900, 2850, 1493, 1350, 1230, 850$ cm⁻¹.

A synthesis of the ligand in aqueous media or under methanol-free condition tested (2.64 g, 43%).

2.2.3. Synthesis of H₂L^{SMe}

This ligand was synthesized according to procedure reported in the literature (2.36 g, 44.1%). MP. 116.8 °C. ¹H NMR: (CDCl₃/250 MHz): δ 7.89 (s, 2H, OH), 7.24 (s, 2H, C₆H₂), 6.93 (s, 2H, C₆H₂), 3.67 (s, 4H, CH₂), 2.76 (s, 4H, CH₂), 2.01 (s, 3H, CH₃), 1.43 (s, 18H, C(CH₃)₃), 1.29 (s, 18H, C(CH₃)₃). IR (KBr): $\nu = 3250, 2975, 2840, 2800, 1495, 1360, 1250, 875$ cm⁻¹.

2.2.4. Synthesis of H₂L^{OH}

A solution of 2,4-di-*tert*-butylphenol (5.0 g, 24.2 mmol), ethanolamine (0.73 ml, 12.1 mmol) and 36% aqueous formaldehyde (4.0 ml, 48.0 mmol) in 10 ml of methanol was stirred and refluxed for 24 h. After cooling the mixture in the freezer overnight, the solvent was removed. The residue was washed repeatedly with little amounts of cold methanol to give the product as a white powder (1.76 g, 29.3%). The product was further purified by recrystallization from dichloromethane/ methanol solvent mixture (2:1). MP. 103.5 °C. ¹H NMR: (CDCl₃/250 MHz): δ 7.24 (s, 2H, C₆H₂), 6.91 (s, 2H, C₆H₂), 3.89 (t, $J = 5$ Hz, 2H, CH₂), 3.79 (s, 4H, CH₂), 2.76 (t, 2H, CH₂), 1.47 (s, 18H, C(CH₃)₃), 1.19 (s, 18H, C(CH₃)₃). IR (KBr): $\nu = 3400, 2960, 2890, 2810, 1470, 1320, 830$ cm⁻¹.

A synthesis of the ligand in aqueous media or under methanol-free condition tested (2.05 g, 34.2%).

2.2.5. Synthesis of H_2L^{OAC}

Acylation of H_2L^{OH} was done according to the procedure reported in the literature [36]. A mixture of acetylchloride (0.18 ml, 2 mmol), H_2L^{OH} (0.497 g, 1 mmol) and 0.0017 g, (0.0016 mmol) of N,N',N'',N''' -tetramethyl-tetra-2,3-pyranoporphyrazinatocopper(II) [$Cu(2,3-tmtppa)]^{4+}$, in 5 ml of dichloromethane was stirred for 4 h at room temperature. Water and *n*-hexane were added to the mixture so that the catalyst was extracted to the water phase and product was left in the organic phase. After removing solvent, the viscous yellowish material cooled in the freezer overnight. The residue was triturated with cold methanol, filtered and washed thoroughly with cold methanol to give the product as a white powder (1.76 g, 29.3%). The product was further purified by recrystallization from a dichloromethane/methanol (2:1) solvent mixture. MP. 136.9 °C. 1H NMR: ($CDCl_3/TMS$ -250 MHz): δ 7.72 (s, 2H, OH), 7.23 (s, 2H, C_6H_2), 6.91 (s, 2H, C_6H_2), 4.27 (s, 2H, CH_2), 3.73 (s, 4H, CH_2), 2.83 (t, 2H, CH_2), 2.17 (s, 3H, CH_3), 1.4 (s, 18H, $C(CH_3)_3$), 1.28 (s, 18H, $C(CH_3)_3$).

^{13}C NMR: ($CDCl_3/TMS$ -250 MHz): δ 152.28 (C=O), 141.46, 123.75, 121.07, 57.47 (Ar CH_2), 51.73 (CH_2), 34.91 ($C(CH_3)_3$), 34.16 ($C(CH_3)_3$), 31.61 ($C(CH_3)_3$), 29.61 ($C(CH_3)_3$), 20.86 (CH_2). IR (KBr): ν = 3420, 2970, 2900, 1720, 1473, 1325, 840 cm^{-1} .

2.2.6. Synthesis of $Cu_2L^{Et_2}$

H_2L^{Et} (0.481 g, 1 mmol) was added to a solution of triethylamine (0.54 g, 10 mmol) in methanol (50 ml). The solution was stirred for 10 min at room temperature. Then $Cu(OAC)_2 \cdot 2H_2O$ (0.199 g, 1 mmol) was added to the solution. The mixture was refluxed for 60 min whereupon a color changed to red brown occurred and some light brown precipitate was formed. The solution was filtered and washed with methanol. Dark-brown crystals were isolated from a dichloromethane/methanol mixture (2:1). Yield = 0.37 g (68.2%). *Anal.* Calc. for $C_{64}H_{98}Cu_2N_2O_4$ (1086.52 g/mol): C, 69.6; H, 8.8; N, 3.7. Found: C, 70.8; H, 9.0; N, 2.6%. UV-Vis in DMF: λ_{max} , nm (ϵ , $M^{-1} cm^{-1}$): 431 (1700), 669 (633). IR (KBr): ν = 2920, 2900, 2850, 1495, 1290, 855 cm^{-1} .

2.2.7. Synthesis of $Cu_2L^{Bu_2}$

H_2L^{Et} (0.509 g, 1 mmol) was added to a solution of triethylamine (0.27 ml, 3 mmol) in methanol (50 ml). The solution was stirred for 10 min at room temperature. Then $Cu(OAC)_2 \cdot 2H_2O$ (0.199 g, 1 mmol) was added to the solution. The mixture was refluxed for 60 min. Meanwhile, the color changed to red brown and some light brown precipitate appeared. The solution was filtered and washed with methanol. Dark-brown crystals were isolated from dichloromethane/ methanol (2:1). Yield = 0.4 g (70.4%). *Anal.* Calc. for $C_{68}H_{106}Cu_2N_2O_4$ (1142.63 g/mol): C, 71.1; H, 9.1; N, 3.0. Found: C, 71.5; H, 9.3; N, 2.4%. UV-Vis in DMF: λ_{max} , nm (ϵ , $M^{-1} cm^{-1}$): 436 (1790), 668 (649). IR (KBr): ν = 2960, 2920, 2860, 1500, 1360, 1220, 840 cm^{-1} .

2.2.8. Synthesis of $Cu_2L^{SMe_2}$

H_2L^{Et} (0.527 g, 1 mmol) was added to a solution of triethylamine (0.27 ml, 3 mmol) in methanol (50 ml). The solution was stirred for 10 min at room temperature. Then $Cu(OAC)_2 \cdot 2H_2O$ (0.199 g, 1 mmol) was added to the solution. The mixture was refluxed for 60 min. Meanwhile, the color changed to red brown and some light brown precipitate appeared. The solution was filtered and washed with methanol. Red-brown crystals were isolated from dichloromethane/methanol (2:1). Yield = 0.41 g (69.2%) *Anal.* Calc. for $C_{66}H_{102}Cu_2N_2O_4S_2$ (1178.70 g/mol): C, 66.7; H, 8.7; N, 2.4. Found: C, 67.3; H, 8.6; N, 2.4%. UV-Vis in DMF: λ_{max} ,

nm (ϵ , $M^{-1} cm^{-1}$): 474 (3050), 703 (580). IR (KBr): ν = 2980, 2850, 2830, 1520, 1370, 1260, 880 cm^{-1} .

2.2.9. Synthesis of $Cu_2L^{OH_2}$

H_2L^{Et} (0.539 g, 1 mmol) was added to a solution of sodium methoxide (0.15 ml, 3 mmol) in methanol (50 ml). The solution was stirred for 10 min at room temperature. Then $Cu(OAC)_2 \cdot 2H_2O$ (0.199 g, 1 mmol) was added to the solution. The mixture was refluxed for 120 min. Meanwhile, the color changed to red brown and some light brown precipitate appeared. The solution was filtered and washed with methanol. Brown crystals were isolated from dichloromethane/ methanol (2:1). Yield = 0.2 g (35.4%) *Anal.* Calc. for $C_{68}H_{102}Cu_2N_2O_8$ (1201.08 g/mol): C, 66.7; H, 8.8; N, 2.3. Found: C, 67.9; H, 8.5; N, 2.3%. UV-Vis in DMF: λ_{max} , nm (ϵ , $M^{-1} cm^{-1}$): 465 (2920), 557 (708). IR (KBr): ν = 2975, 2820, 2800, 1480, 1300, 820 cm^{-1} .

3. Results and discussion

The synthesis of the ligands H_2L^{Et} , H_2L^{Bu} , H_2L^{SMe} and H_2L^{OH} is based on a single-step Mannich condensation of the amine with formaldehyde, and 2,4-di-*tert*-butyl phenol. Dinuclear copper complexes were easily formed in good yields by refluxing methanolic solutions of the ligands with copper acetate and a base (sodium methoxide or triethylamine). In the case of H_2L^{OH} , an insoluble polymeric material was formed. To prevent polymerization of this complex through hydroxyl side arm of the mentioned ligand, the hydroxyl group was selectively protected in the presence of phenol groups by acylation before reaction with copper salt. The ester group in the pendant arm(H_2L^{OH}) seems to be hydrolyzed to hydroxyl via nucleophilic attack of water during complexation.

In IR spectra of most complexes, the strong and sharp band at frequencies higher than 3000 cm^{-1} for the ν_{OH} stretch of ligands were disappeared, proving the coordination of phenol groups to the metal.

3.1. X-ray data collection and structure determination of $Cu_2L^{Et_2}$, $Cu_2L^{Bu_2}$, $Cu_2L^{SMe_2}$ and $Cu_2L^{OH_2}$

Dark brown crystals of $Cu_2L^{Et_2}$, $Cu_2L^{Bu_2}$, $Cu_2L^{SMe_2}$ and $Cu_2L^{OH_2}$ for X-ray analysis were obtained from methanol/dichloromethane (1:2) solution. Details of data collection and refinement of the structures are summarized in Table 1. Selected bond lengths and angles for $Cu_2L^{Et_2}$, $Cu_2L^{Bu_2}$, $Cu_2L^{SMe_2}$ and $Cu_2L^{OH_2}$ are presented in Tables 2–5. A complete listing of bond lengths and angles for these complexes can be found in the Supplementary material.

All compounds reported in this study are of the general formula $[L_2Cu_2]^0$. Complexes with ligands having alkyl groups attached to the central nitrogen consist of two phenolato bridged square planar copper centers in a N_3O coordination environment showing a considerable tetrahedral distortion. Compounds carrying side chains with an additional coordinating function ($Cu_2L^{SMe_2}$ and $Cu_2L^{OH_2}$) form pentacoordinated species with distorted square pyramidal geometry binding the additional donor in an apical position.

Structural analysis of the reported dimeric complexes revealed short Cu...Cu distances being 2.6710(4), 2.6800(4), 2.8157(2) and 2.7206(10) Å for $Cu_2L^{Et_2}$, $Cu_2L^{Bu_2}$, $Cu_2L^{SMe_2}$, $Cu_2L^{OH_2}$, respectively. The Cu...Cu distances found in $Cu_2L^{Et_2}$, $Cu_2L^{Bu_2}$ are, to the best of our knowledge, the shortest which have ever been detected in bis(μ -phenoxo)dicopper(II) complexes to date. These short distances arise from a distinct folding of the two square planar moieties along the O–O vector in the central Cu_2O_2 ring. The calculated angle between the two mean planes containing the Cu ion and the two phenoxo oxygen atoms is about 63° in both cases (63.7° and 62.2° for $Cu_2L^{Et_2}$ and $Cu_2L^{Bu_2}$, respectively) which allows the Cu ions to come very close.

Table 1Crystal data and structure refinement for $\text{Cu}_2\text{L}^{\text{Et}_2}$, $\text{Cu}_2\text{L}^{\text{Bu}_2}$, $\text{Cu}_2\text{L}^{\text{SMe}_2}$ and $\text{Cu}_2\text{L}^{\text{OH}_2}$.

Identification code	$\text{Cu}_2\text{L}^{\text{Et}_2}$	$\text{Cu}_2\text{L}^{\text{Bu}_2}$	$\text{Cu}_2\text{L}^{\text{SMe}_2}$	$\text{Cu}_2\text{L}^{\text{OH}_2}$
Empirical formula	$\text{C}_{64}\text{H}_{98}\text{Cu}_2\text{N}_2\text{O}_4$	$\text{C}_{68}\text{H}_{106}\text{Cu}_2\text{N}_2\text{O}_4$	$\text{C}_{66}\text{H}_{102}\text{Cu}_2\text{N}_2\text{O}_4\text{S}_2$	$\text{C}_{64}\text{H}_{98}\text{Cu}_2\text{N}_2\text{O}_6$
Formula weight	1086.52	1142.63	1178.70	1118.52
Temperature (K)	100(2)	100(2)	100(2)	100(2)
Wavelength (Å)	0.71073	0.71073	0.71073	0.71073
Crystal system	orthorhombic	monoclinic	triclinic	orthorhombic
Space group	<i>Pcca</i>	<i>P2₁/c</i>	<i>P</i> $\bar{1}$	<i>Pcca</i>
<i>Unit cell dimensions</i>				
<i>a</i> (Å)	28.995(2)	16.558(2)	13.7277(10)	28.891(6)
<i>b</i> (Å)	10.9773(6)	19.664(2)	14.3528(11)	10.817(2)
<i>c</i> (Å)	19.0806(9)	21.441(3)	18.7074(14)	19.128(4)
β (°)	90.00	109.072(3)	82.911(2)	90.00
Volume (Å ³)	6073.1(6)	6597.9(14)	3272.7(4)	5978(2)
<i>Z</i>	4	4	2	4
Calculated density (Mg/m ³)	1.188	1.150	1.196	1.243
Absorption coefficient (mm ⁻¹)	0.746	0.690	0.759	0.762
<i>F</i> (0 0 0)	2344	2472	1268	2408
Crystal size (mm)	0.60 × 0.30 × 0.18	0.05 × 0.05 × 0.04	0.06 × 0.06 × 0.04	0.08 × 0.07 × 0.04
Theta range for data collection (°)	3.00–32.50	2.01–31.00	1.75–35.00	2.13–23.51
Index ranges	–43 ≤ <i>h</i> ≤ 43 –16 ≤ <i>k</i> ≤ 16 –28 ≤ <i>l</i> ≤ 28	–23 ≤ <i>h</i> ≤ 23 –28 ≤ <i>k</i> ≤ 28 –31 ≤ <i>l</i> ≤ 31	–22 ≤ <i>h</i> ≤ 22 –23 ≤ <i>k</i> ≤ 23 –30 ≤ <i>l</i> ≤ 30	–32 ≤ <i>h</i> ≤ 32 –12 ≤ <i>k</i> ≤ 12 –21 ≤ <i>l</i> ≤ 21
Reflections collected/unique	100 874/10 975	165 828/21 005	199 490/28 692	76 923/4382
Data/restraints/parameters	[<i>R</i> _{int} = 0.0438] 10 975/10/360	[<i>R</i> _{int} = 0.0519] 21 005/19/737	[<i>R</i> _{int} = 0.0363] 28 692/7/721	[<i>R</i> _{int} = 0.1586] 4382/20/366
Goodness-of-fit on <i>F</i> ²	1.018	1.109	1.067	1.106
Final <i>R</i> indices [<i>I</i> > 2σ(<i>I</i>)]	<i>R</i> ₁ = 0.0454, <i>wR</i> ₂ = 0.1117	<i>R</i> ₁ = 0.0392, <i>wR</i> ₂ = 0.1003	<i>R</i> ₁ = 0.0277, <i>wR</i> ₂ = 0.0722	<i>R</i> ₁ = 0.0504, <i>wR</i> ₂ = 0.1140
<i>R</i> indices (all data)	<i>R</i> ₁ = 0.0575, <i>wR</i> ₂ = 0.1248	<i>R</i> ₁ = 0.0567, <i>wR</i> ₂ = 0.1172	<i>R</i> ₁ = 0.0396, <i>wR</i> ₂ = 0.0809	<i>R</i> ₁ = 0.0567, <i>wR</i> ₂ = 0.1172
Largest difference peak and hole (e Å ⁻³)	0.588 and –1.402	1.380 and –0.596	0.658 and –0.481	0.579 and –0.484

Table 2Selected bond lengths (Å) and angles (°) for $\text{Cu}_2\text{L}^{\text{Et}_2}$.

Identification code	$\text{Cu}_2\text{L}^{\text{Et}_2}$
Cu(1)–O(17)	1.8513(10)
Cu(1)–O(1)	1.9373(9)
Cu(1)–N(9)	2.0177(14)
Cu(1)–Cu(1)#1	2.6710(4)
Cu(1)#1–O(1)	2.0268(12)
O(1)–Cu(1)–N(9)	94.33(5)
O(1)#1–Cu(1)–O(17)	94.59(5)
Cu(1)–O(1)–Cu(1)#1	84.69(4)
O(17)–Cu(1)–O(1)	168.52(5)
O(1)#1–Cu(1)–O(1)	75.10(5)
O(17)–Cu(1)–N(9)	97.13(5)
O(1)#1–Cu(1)–N(9)	155.14(5)
O(1)–Cu(1)–Cu(2)	49.07(4)
O(17)–Cu(1)–Cu(2)	126.35(5)
N(9)–Cu(1)–Cu(2)	110.04(4)
O(1)#1–Cu(1)–Cu(2)	46.24(3)

Symmetry transformations used to generate equivalent atoms:

#1 – *x* + 1/2, –*y*, *z* for $\text{Cu}_2\text{L}^{\text{Et}_2}$.

We have also reported a similar bisphenoxo compound, $\text{L}^{\text{hf}_2}\text{Cu}_2$ ($\text{H}_2\text{L}^{\text{hf}} = N,N$ -bis(3,5-di-*tert*-butyl-2-hydroxybenzyl)-2-(amino-methyl) tetrahydrofuran), with a Cu...Cu separation of 2.766 Å and two related complexes of amine-bis(phenolate) ligands bearing methoxyethyl and methylthiophen arms $\text{L}^{\text{m}_2}\text{Cu}_2$ and $\text{L}^{\text{s}_2}\text{Cu}_2$ with Cu...Cu distances of 2.7868(6) and 2.7187(8) Å [23,37].

For other phenoxo bridged binuclear copper complexes [38–40,22], larger separations of the copper centers of about 3 Å have been observed.

The Cu1–O1–Cu1 bridge angles within the central four-membered Cu_2O_2 ring are 84.69(4), 85.20(4), 89.94(2) and 86.93(9) deg in $\text{Cu}_2\text{L}^{\text{Et}_2}$, $\text{Cu}_2\text{L}^{\text{Bu}_2}$, $\text{Cu}_2\text{L}^{\text{SMe}_2}$ and $\text{Cu}_2\text{L}^{\text{OH}_2}$, respectively and the O1–Cu1–O1 angles are at 75.10(5), 75.92(4), 73.70(2) and

75.06(11). These angles are smaller than corresponding angles reported in Refs. [38–40,22].

In $\text{Cu}_2\text{L}^{\text{Et}_2}$ (Fig. 1), the Cu1–O1, Cu1–O17 and Cu1–N9 bonds are 1.9373(9), 1.8513(10) and 2.0177(14) Å, respectively. The O17–Cu1–O1 fragment is almost linear, the corresponding valence angle being 168.52(5)°. The sum of angles around the bridging phenoxo oxygen atoms is about 339 deg (for O1) which proves it to be pyramidal rather than planar (Table 2).

The Cu1–O1, Cu1–O57 and Cu1–N49 bonds in $\text{Cu}_2\text{L}^{\text{Bu}_2}$ (Fig. 2) are at of typical values of 2.0335(11), 1.8457(11) and 2.0290(13) Å, respectively. The sum of angles around bridge oxygen with the value of 336.23° proves the pyramidal coordination rather than planar for O1 (Table 3).

The Cu1–O41, Cu1–O57, Cu1–N49 and Cu1–S76 bonds of $\text{Cu}_2\text{L}^{\text{SMe}_2}$ are 1.9632(6), 1.8796(7), 2.0542(7) and 2.6905(3) Å,

Table 4Selected bond lengths (Å) and angles (°) for $\text{Cu}_2\text{L}^{\text{SMe}_2}$.

Identification code	$\text{Cu}_2\text{L}^{\text{SMe}_2}$
Cu(1)–O(41)	1.9632(6)
Cu(1)–N(49)	2.0542(7)
Cu(1)–Cu(2)	2.8157(2)
Cu(2)–O(1)	1.9608(6)
O(1)–Cu(1)–N(49)	148.35(3)
O(57)–Cu(1)–O(41)	165.62(3)
Cu(1)–O(1)–Cu(2)	89.94(2)
O(17)–Cu(2)–O(41)	91.50(3)
O(41)–Cu(2)–O(1)	73.70(2)
O(17)–Cu(2)–N(9)	96.17(3)
O(41)–Cu(1)–N(49)	93.84(3)
O(1)–Cu(2)–Cu(1)	45.925(18)
O(17)–Cu(2)–Cu(1)	116.41(2)
N(9)–Cu(2)–Cu(1)	109.21(2)
O(41)–Cu(2)–Cu(1)	44.203(17)
Cu(1)–S(76)	2.6905(3)
Cu(2)–S(36)	2.6669(3)
O(17)–Cu(2)–S(36)	102.16(2)
O(41)–Cu(2)–S(36)	121.124(18)
S(36)–Cu(2)–N(9)	83.46(2)
N(49)–Cu(1)–S(76)	83.59(2)

Table 5Selected bond lengths (Å) and angles (°) for $\text{Cu}_2\text{L}^{\text{OH}_2}$.

Identification code	$\text{Cu}_2\text{L}^{\text{OH}_2}$
Cu(1)–O(17)	1.848(2)
Cu(1)–O(1)	1.932(2)
Cu(1)–N(9)	2.041(3)
Cu(1)–Cu(1)#1	2.7206(10)
Cu(1)#1–O(1)	2.022(2)
O(1)–Cu(1)–N(9)	93.70(11)
O(1)#1–Cu(1)–O(17)	93.37(10)
Cu(1)–O(1)–Cu(1)#1	86.93(9)
O(17)–Cu(1)–O(1)	168.40(10)
O(1)#1–Cu(1)–O(1)	75.06(11)
O(17)–Cu(1)–N(9)	97.01(11)
O(1)#1–Cu(1)–N(9)	151.02(11)
O(1)–Cu(1)–Cu(1)#1	47.91(7)
O(17)–Cu(1)–Cu(1)#1	123.65(8)
N(9)–Cu(1)–Cu(1)#1	107.85(8)
O(28)–Cu(1)–O(1)#1	139.67(12)
Cu(1)–O(28)	2.425(5)

Symmetry transformations used to generate equivalent atoms:

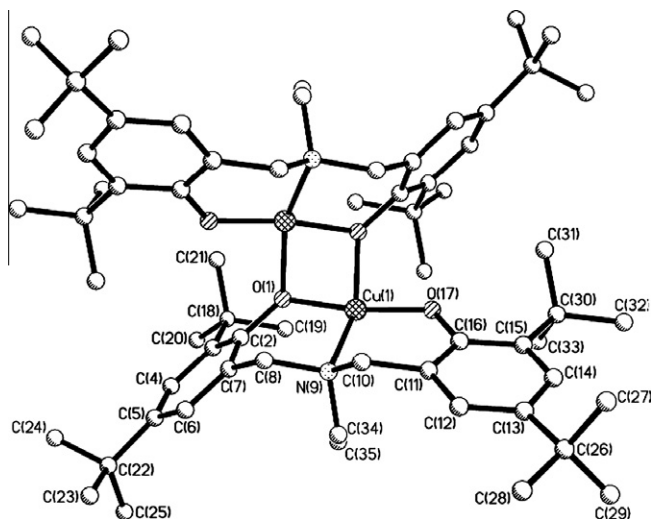
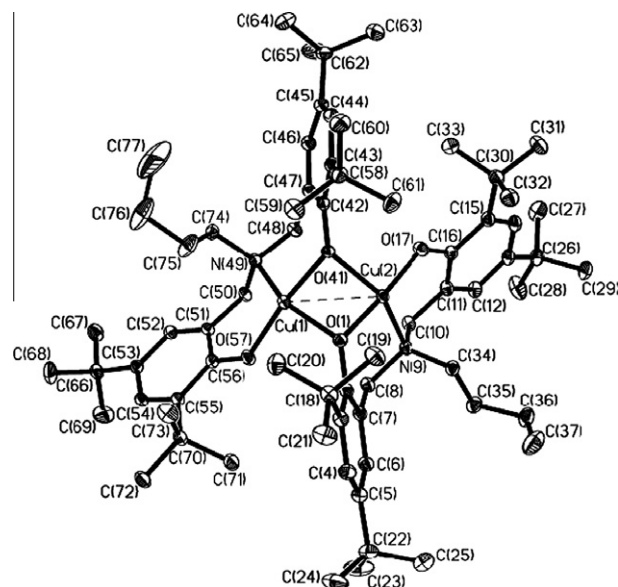
#1 – $x + 3/2, -y + 1, z$ for $\text{Cu}_2\text{L}^{\text{OH}_2}$.

respectively (Fig. 3). The geometrical parameters τ for this complex is 0.29 for Cu(1) and 0.22 Cu(2), respectively (Table 2). Comparing these τ values with corresponding values for ideal trigonal bipyramid ($\tau = 1$) and square pyramidal ($\tau = 0$) suggest that this complex has a square-pyramidal geometry.

The Cu1...Cu2 distance at 2.8157(2) Å within the dimer $\text{Cu}_2\text{L}^{\text{SMe}_2}$ is longer than those reported for the $\text{Cu}_2\text{L}^{\text{Et}_2}$ and $\text{Cu}_2\text{L}^{\text{Bu}_2}$ analogs. The central Cu_2O_2 ring has also a different geometry due to the O41–Cu2–O1 and Cu1–O1–Cu2 angles being 73.70(2) and 89.94(2)°, respectively.

The sum of angles around the bridging oxygen atom O41 with a value of 342.47° proves a slightly more planar coordination mode compared to $\text{Cu}_2\text{L}^{\text{Et}_2}$ and $\text{Cu}_2\text{L}^{\text{Bu}_2}$.

The architecture of $\text{Cu}_2\text{L}^{\text{OH}_2}$ is similar to that of $\text{Cu}_2\text{L}^{\text{SMe}_2}$. The two copper centers form a distorted square pyramidal coordination environment with τ value of 0.29 (Fig. 4). The $\text{CH}_2\text{CH}_2\text{OH}$ group was found to be disordered and only about 55% of the side arms are loosely bound to the copper centers and about 45% are not coordinated. The O1–Cu1–O17 fragment is almost linear, the correspond-

**Fig. 1.** ORTEP diagram and atom labeling scheme for complex $\text{Cu}_2\text{L}^{\text{Et}_2}$.

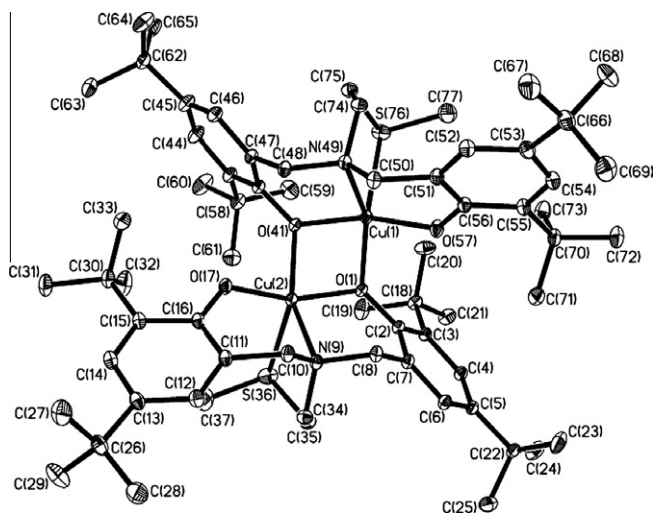


Fig. 3. ORTEP diagram and atom labeling scheme for complex $\text{Cu}_2\text{L}^{\text{SMe}_2}$.

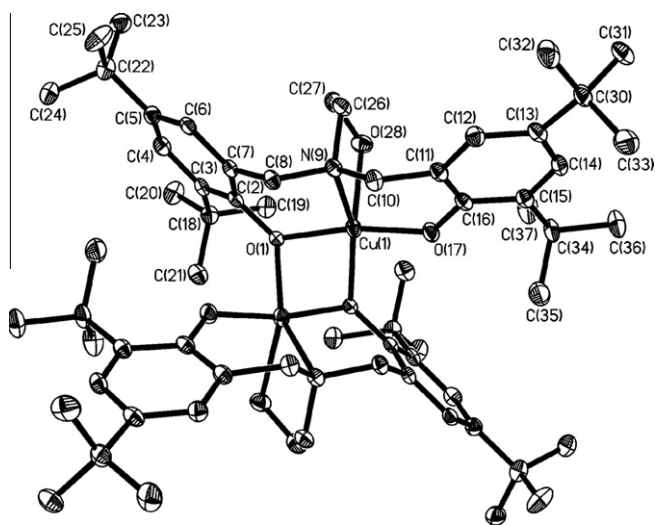


Fig. 4. ORTEP diagram and atom labeling scheme for complex $\text{Cu}_2\text{L}^{\text{OH}_2}$.

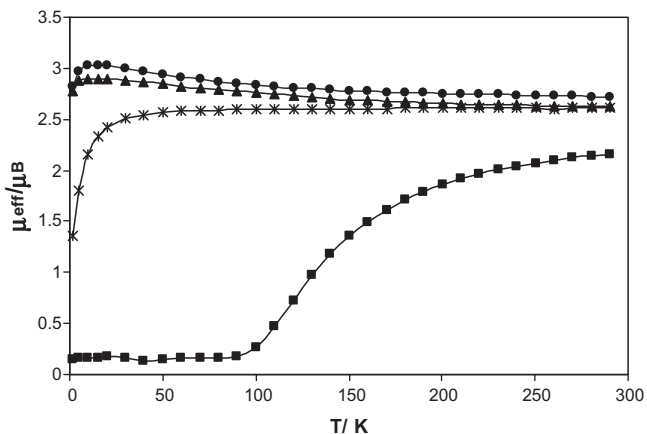


Fig. 5. Magnetic measurements for complexes $\text{Cu}_2\text{L}^{\text{Et}_2}$ (▲), $\text{Cu}_2\text{L}^{\text{Bu}_2}$ (●), $\text{Cu}_2\text{L}^{\text{SMe}_2}$ (■) and $\text{Cu}_2\text{L}^{\text{OH}_2}$ (*).

let ground state ($S = 1$). Simulation of the magnetic moment for this complex yields $J = +26.62 \text{ cm}^{-1}$, $g = 2.16$.

In the case of $\text{Cu}_2\text{L}^{\text{Bu}_2}$ a similar behavior is observed. The effective magnetic moment (μ_{eff}) for this complex decreases from $3.02 \mu_{\text{B}}$ at 10 K to $2.72 \mu_{\text{B}}$ at 290 K (Fig. 5). This complex appears to have triplet ground state ($S = 1$) due to ferromagnetic coupling between two copper centers. Simulation of the magnetic moment yields $J = +38.66 \text{ cm}^{-1}$, $g = 2.05$.

The magnetic behavior of $\text{Cu}_2\text{L}^{\text{SMe}_2}$ with temperature is completely different of $\text{Cu}_2\text{L}^{\text{Et}_2}$, $\text{Cu}_2\text{L}^{\text{Bu}_2}$ complexes. The effective magnetic moment per molecule (μ_{eff}) in this complex decreases to $0.20 \mu_{\text{B}}$ at 2–90 K from the maximum value of 2.2 at 290 K (Fig. 5). It demonstrates that there is antiferromagnetic coupling between the two copper centers leading to a singlet ground state ($S = 0$) (Fig. 5). Simulation of the magnetic moment yields $J = -65.88 \text{ cm}^{-1}$, $g = 2.04$.

The magnetic behavior of $\text{Cu}_2\text{L}^{\text{OH}_2}$ is similar to that of $\text{Cu}_2\text{L}^{\text{SMe}_2}$. The effective magnetic moment (μ_{eff}) with the constant value of $2.60 \mu_{\text{B}}$ at 30–290 K decreases to $1.36 \mu_{\text{B}}$ along with the drop in temperature to 2 K (Fig. 5). This behavior can be attributed to a weak antiferromagnetic coupling between two copper centers with a singlet ground state ($S = 0$). Simulation of the magnetic moment yields $J = -2.77 \text{ cm}^{-1}$, $g = 2.14$.

It is well known that in dinuclear copper(II) complexes with di- μ -hydroxo and di- μ -alkoxo bridges, the singlet-triplet (S - T) energy gap J correlates with the bridging oxygen Cu–O–Cu angle (α). The following formula has been established for these cases.[41].

$$J(\text{cm}^{-1}) = -74\alpha + 7270 \quad (2)$$

If α is about 97.5° , J is equal to zero and the systems are uncoupled. If α is smaller than 97.5° , the complex will show a ferromagnetic character and a triplet ground state. A bridging angle larger than 97.5° leads to an antiferromagnetically coupled system with a diamagnetic ground state ($S = 0$). A similar relationship was found for bis-phenoxide bridged macrocyclic dicopper(II) complexes [42].

$$2J(\text{cm}^{-1}) = -31.95\alpha + 2462 \quad (3)$$

Considering the relationship (Eqs. (2)–(5)) between the singlet-triplet energy gap and the Cu–O(Ph)–Cu angle (α) allows to find the effect of structural factors of our complexes on the exchange interactions between copper centers [42–46].

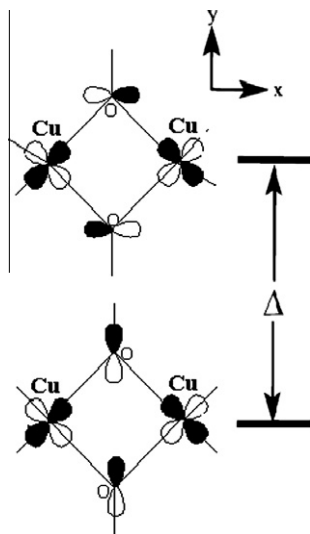
$$2J = E_T - E_S \quad (4)$$

$$J = 2\kappa - (\varepsilon_1 - \varepsilon_2)^2/U \quad (5)$$

where 2κ and $(\varepsilon_1 - \varepsilon_2)^2$ terms describe the ferro- and antiferromagnetic contributions, respectively. The variation of α and Cu...Cu distances affects the overlap of $\text{Cu}(3d_{xy})/\text{O}(2p)$ orbitals and therefore changes $\varepsilon_1 - \varepsilon_2$ (the energy difference between $\text{Cu}(3d_{xy})/\text{O}(2p_x)$ and $\text{Cu}(3d_{xy})/\text{O}(2p_y)$) orbitals (Scheme 2). In $\text{Cu}_2\text{L}^{\text{Et}_2}$, $\text{Cu}_2\text{L}^{\text{Bu}_2}$ complexes, the small α of 84.69° and 85.20° and Cu...Cu distances of 2.67 and 2.68 Å, caused $\varepsilon_1 - \varepsilon_2$ term to become negligible. Consequently, the ferromagnetic term 2κ dominates and complexes show a ferromagnetic coupling with a triplet ground state.

The longer distance of $\text{Cu1} \cdots \text{Cu2}$ of 2.8157 Å, the larger value of bridge angle ($\alpha = 89.76^\circ$) and also more planarity of Cu_2O_2 core in $\text{Cu}_2\text{L}^{\text{SMe}_2}$ due to the coordination of thiomethyl groups to copper centers increase the antiferromagnetic contribution in this complex.

The coupling constant value in $\text{Cu}_2\text{L}^{\text{SMe}_2}$ is considerably low compared to those reported ($|J| > 100 \text{ cm}^{-1}$) for similar phenolato bridge copper complexes [38–40,22]. It can be attributed to the lower bridge angle ($\alpha < 97.5^\circ$) of this complex in comparison to others and more effective ferromagnetic contribution to the overall magnetic moment of the complex.



Scheme 2. Magnetic molecular orbitals for Cu–O(Ph)–Cu framework [42].

We already showed for a similar copper dimer that coordination of an amine-bis(phenol) ligand which bears a tetrahydrofuran side arm affects α , Cu...Cu separation and consequently exchange coupling (Cu...Cu separation of 2.766 Å, $\alpha = 88^\circ$, $J = -12.0 \text{ cm}^{-1}$) [23]. A comparison of these values with the corresponding ones for phenolato bridged copper complex of bis(phenol) amine ligand with an uncoordinated thiophene arm (Cu...Cu separation of 2.7187 Å, $\alpha = 89.23^\circ$, $J = 17.94 \text{ cm}^{-1}$) confirms the influence of side arm coordination on structural parameters and consequently magnetic properties [23,37].

The smaller value of α in $\text{Cu}_2\text{L}^{\text{OH}_2}$ ($\alpha = 86.93$) compared to $\text{Cu}_2\text{L}^{\text{SMe}_2}$ caused higher ferromagnetic contribution in the final singlet–triplet (S – T) energy gap J ($J = -2.77 \text{ cm}^{-1}$). It demonstrates that in this complex, ferromagnetic term 2κ is nearly equal to anti-ferromagnetic term $(\varepsilon_1 - \varepsilon_2)^2/U$. Indeed the small angle of $\alpha = 86.93$ for this complex is almost the crossover point from anti-ferromagnetic to ferromagnetic behavior.

Variation of dihedral angle between two adjacent CuO_2 planes (δ) affects $\varepsilon_1 - \varepsilon_2$. The small dihedral angles between two CuO_2 planes in $\text{Cu}_2\text{L}^{\text{Et}_2}$, $\text{Cu}_2\text{L}^{\text{Bu}_2}$, $\text{Cu}_2\text{L}^{\text{OH}_2}$, $\text{Cu}_2\text{L}^{\text{SMe}_2}$ (63.71, 62.2, 56.18 and 59.72, respectively) are indicative for a considerable distortion from the coplanarity of the two square planes and hence the two $d_{x^2-y^2}$ magnetic orbitals. It caused the decreasing of $\varepsilon_1 - \varepsilon_2$ and the observed ferromagnetic contribution to the overall exchange interactions. The low value of coupling constant J in $\text{Cu}_2\text{L}^{\text{SMe}_2}$ can be attributed to this criteria.

The sum of the angles at the bridging phenoxide oxygen atoms are lower than 360° indicating a pyramidal oxygen binding mode which consequently increases the contribution of the ferromagnetic (2κ) term.

3.3. Electrochemistry

Cyclic and differential pulse voltammograms (CV and DPV) of complexes $\text{Cu}_2\text{L}^{\text{Et}_2}$, $\text{Cu}_2\text{L}^{\text{Bu}_2}$, $\text{Cu}_2\text{L}^{\text{SMe}_2}$ and $\text{Cu}_2\text{L}^{\text{OH}_2}$ were recorded in CH_2Cl_2 solutions containing 0.1 M $[(n\text{Bu})_4\text{N}]\text{ClO}_4$ as supporting electrolyte. Prior to the measurement, the GC electrode was polished with 0.1 μm alumina powder and washed with distilled water. The voltage scan rate was set at 50 mV s^{-1} . The solutions were deoxygenated by bubbling nitrogen gas through them for 10 min. Ferrocene was added as an internal standard and potentials were referenced versus the ferrocenium/ferrocene couple (Fc^+/Fc).

The CV and DPV voltammograms observed with $\text{Cu}_2\text{L}^{\text{Et}_2}$, $\text{Cu}_2\text{L}^{\text{SMe}_2}$ and $\text{Cu}_2\text{L}^{\text{OH}_2}$ revealed two oxidations with a similar small difference in their redox potentials, and three oxidations for $\text{Cu}_2\text{L}^{\text{Bu}_2}$ (Table 6 and Fig. 6). The similarity of E^{ox} values for all complexes in the range of 0.5–1.0 V suggests the same oxidation

Table 6

Electrode potentials (in V) for oxidation and reduction of complexes $\text{Cu}_2\text{L}^{\text{Et}_2}$, $\text{Cu}_2\text{L}^{\text{Bu}_2}$, $\text{Cu}_2\text{L}^{\text{SMe}_2}$ and $\text{Cu}_2\text{L}^{\text{OH}_2}$ measured at ambient temperature in CH_2Cl_2 solutions and referenced vs. the Fc^+/Fc couple.

Complex	E_{red}/V	E_1^{ox}/V	E_2^{ox}/V	E_3^{ox}/V
$\text{Cu}_2\text{L}^{\text{Et}_2}$	–	0.42 ^b	0.96 ^a	–
$\text{Cu}_2\text{L}^{\text{Bu}_2}$	–	0.50 ^b	0.73 ^a	1.01 ^a
$\text{Cu}_2\text{L}^{\text{SMe}_2}$	–	0.39 ^b	0.79 ^b	–
$\text{Cu}_2\text{L}^{\text{OH}_2}$	–	0.41 ^b	1.04 ^b	–

^a Irreversible reaction, peak potential is given.

^b Electrochemical quasi-reversible reaction.

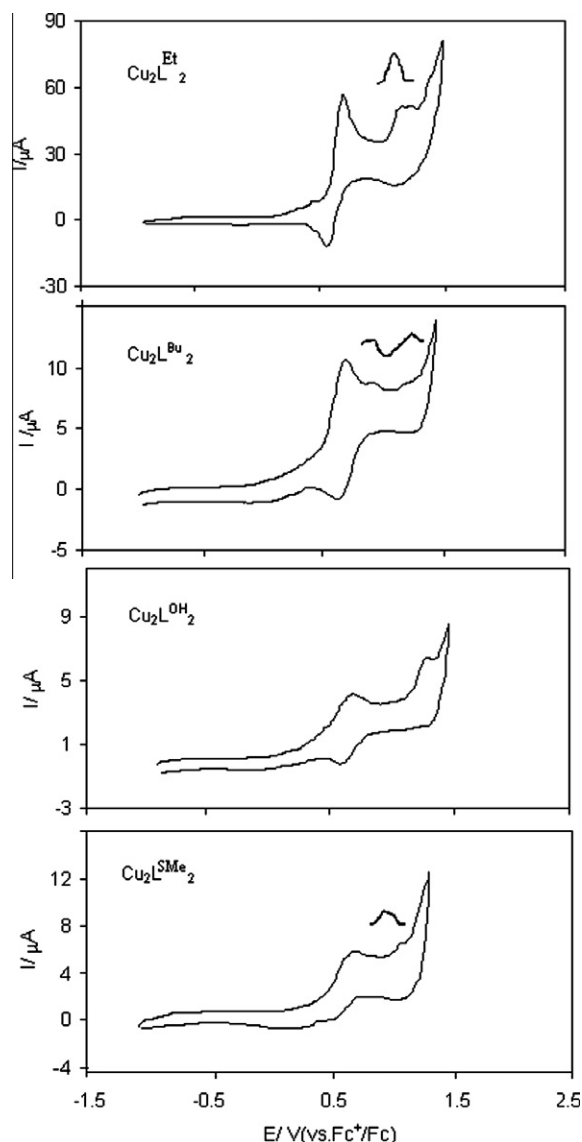


Fig. 6. Cyclic and differential pulse voltammograms of $\text{Cu}_2\text{L}^{\text{Et}_2}$, $\text{Cu}_2\text{L}^{\text{Bu}_2}$, $\text{Cu}_2\text{L}^{\text{SMe}_2}$ and $\text{Cu}_2\text{L}^{\text{OH}_2}$ in CH_2Cl_2 at room temperature.

mechanism for all complexes. As the further oxidation of copper (II) redox process occurs at higher redox potentials, these redox processes are probably attributed to the ligand centered redox processes in which phenolate group yields phenoxyl radical in the complex, but there is no direct evidence available yet.

These ligand-centered voltammograms are electrochemically quasi-reversible, based on deviation of ΔE_p from 1 (ΔE_p is the separation of the oxidation and reduction peaks; the value of ΔE_p for reversible peaks is 1).

These complexes do not exhibit any metal-centered voltammograms in the potential range due to the reduction of copper(II) center.

4. Conclusion

We have thus prepared bis(μ -phenoxo)dycopper(II) complexes with [ONXO]-donor tripodal ligands containing bis(phenol) amine modified with different side arms.

Electrochemical oxidation of these complexes yielded the corresponding Cu(II)-phenoxyl radical species.

Magnetostructural studies of complexes display a range of interesting effects due to the effect of coordinated versus noncoordinated pendant arms on the magnetic properties of these complexes.

The small Cu...Cu separations and Cu–O(Ph)–Cu bridging angles of these complexes compared to other similar bis(μ -phenoxo)dycopper(II) compounds reported in the literature make them unique.

$\text{Cu}_2\text{L}^{\text{SMe}_2}$ and $\text{Cu}_2\text{L}^{\text{OH}_2}$ show a remarkably weak antiferromagnetism while $\text{Cu}_2\text{L}^{\text{Et}_2}$ and $\text{Cu}_2\text{L}^{\text{Bu}_2}$ exhibit ferromagnetic exchange interactions.

Structural changes (most importantly Cu...Cu distance, Cu–O(Ph)–Cu angle changes) were induced by variations of the side arms of the amine-bis(phenol) ligand, which in turn affects whether a diamagnetic ground state ($S=0$) or a triplet state ($S=1$) is preferred.

Acknowledgments

Authors are grateful to the Institute for Advanced Studies in Basic Sciences (IASBS) and Max-Planck-Institute for Bioinorganic Chemistry. E. Safaei gratefully acknowledges the support by the Institute for Advanced Studies in Basic Sciences (IASBS) Research Council under Grant No. G2011IASBS127. Thanks are due to Mr. Andreas Göbels and Mrs. Heike Schucht (MPI-BAC) for their skillful technical assistance.

Appendix A. Supplementary material

CCDC 799217, 799218, 799219 and 799220 contain the supplementary crystallographic data for $\text{Cu}_2\text{L}^{\text{Et}_2}$, $\text{Cu}_2\text{L}^{\text{Bu}_2}$, $\text{Cu}_2\text{L}^{\text{SMe}_2}$ and $\text{Cu}_2\text{L}^{\text{OH}_2}$, respectively. These data can be obtained free of charge from The Cambridge Crystallographic Data Centre via www.ccdc.cam.ac.uk/data_request/cif. Supplementary data associated with this article can be found, in the online version, at doi:10.1016/j.ica.2011.04.048.

References

- [1] R.H. Holm, P. Kennepohl, E. Solomon, *Chem. Rev.* 96 (1996) 2239.
- [2] H. Sigel, A. Sigel, *Metal Ions in Biological Systems*, vol. 30, Marcel Dekker, New York, 1994.
- [3] K.D. Karlin, *Science* 261 (1993) 701.
- [4] H.C. Liang, M. Dahan, K.D. Karlin, *Science* 3 (1999) 168.
- [5] J. Stubbe, W.A. van der Donk, *Chem. Rev.* 98 (1998) 705.
- [6] D.J. Kosman, in: R. Lontie (Ed.), *Copper Proteins and Copper Enzymes*, vol. 2, CRC Press, Boca Raton, FL, 1985, pp. 1–26.
- [7] J.W. Whittaker, *Chem. Rev.* 103 (2003) 2347.
- [8] J.W. Whittaker, in: K.D. Karlin, Z. Tyeklar (Eds.), *Bioinorganic Chemistry of Copper*, Chapman Hall, New York, 1993, pp. 447–458.
- [9] M.J. McPherson, M.R. Parsons, R.K. Spooner, C.M. Wilmot, Galactose oxidase, in: K. Wieghart, T.L. Poulos, R. Huber, A. Messerschmidt (Eds.), *Handbook of Metalloproteins*, vol. 2, Wiley, New York, 2001, pp. 1245–1257.
- [10] E.I. Solomon, U.M. Sundaram, Timothy E. Machonkin, *Chem. Rev.* 96 (1996) 2563–2605.
- [11] N. Ito, S.E.V. Phillips, K.D.S. Yadav, P.F. Knowles, *J. Mol. Biol.* 238 (1994) 794.
- [12] Brian A. Jazdzewski, William B. Tolman, *Coord. Chem. Rev.* 200–202 (2000) 633.
- [13] P. Chaudhuri, M. Hess, U. Flörke, K. Wieghardt, *Angew. Chem., Int. Ed.* 37 (1998) 2217.
- [14] F. Michel, F. Thomas, S. Hamman, C. Philouze, E. Saint-Aman, J.L. Pierre, *Eur. J. Inorg. Chem.* (2006) 3684.
- [15] A.L. Philibert, F. Thomas, C. Philouze, S. Hamman, E. Saint-Aman, J.L. Pierre, *Chem. Eur. J.* 9 (2003) 3803.
- [16] Brian Turner, Shawn Swavey, *Inorg. Chem. Commun.* 10 (2007) 209.
- [17] L. Rodriguez, E. Labisbal, A. Sousa-Pedrares, J.A. Garcia-Vazquez, J. Romero, M.L. Duran, J.A. Real, A. Sousa, *Inorg. Chem.* 45 (2006) 7903.
- [18] S. Itoh, M. Taki, S. Fukuzumi, *Coord. Chem. Rev.* 198 (2000) 3.
- [19] B.A. Jazdzewski, W.B. Tolman, *Coord. Chem. Rev.* 200 (2000) 633.
- [20] R.N. Patel, N. Singh, K.K. Shukla, V.L.N. Gundla, U.K. Chauhan, *J. Inorg. Biochem.* 99 (2005) 651.
- [21] R. Gupta, S. Mukherjee, R. Mukherjee, *J. Chem. Soc., Dalton Trans.* (1999) 4025.
- [22] S. Mukhopadhyay, D. Mandal, P.B. Chatterjee, C. Desplanches, J.-P. Sutter, R.J. Butcher, M. Chaudhury, *Inorg. Chem.* 43 (2004) 8501.
- [23] E. Safaei, T. Weyhermüller, E. Bothe, K. Wieghardt, Phalguni Chaudhuri, *Eur. J. Inorg. Chem.* 16 (2007) 2334.
- [24] H. Saimiy, Y. Sunatsuki, M. Kojima, S. Kashino, T. Kambe, M. Hirotsu, H. Akashi, K. Nakajima, T. Tokii, *J. Chem. Soc., Dalton Trans.* (2002) 3737.
- [25] P. Jeffrey Hay, J.C. Thibeault, R. Hoffmann, *J. Am. Chem. Soc.* 97 (1975) 4884.
- [26] C.J. O'Connor, *Prog. Inorg. Chem.* 29 (1982) 203.
- [27] R.C. Weast, M.J. Astle, *CRC Handbook of Chemistry and Physics*, CRC Press Inc., Boca Raton, Florida, 1979.
- [28] E. Bill, available from <http://www.mpi-muelheim.mpg.de/bac/logins/bill/julX_en.php>, 2008.
- [29] E. Bill, The LAPACK Linear Algebra Package is written in Fortran77 and provides routines for solving systems of simultaneous linear equations, least-squares solutions of linear systems of equations, eigenvalue problems, and singular value problems. The routines are available at <<http://www.netlib.org/lapack/>>, 2008.
- [30] V.I. Lebedev, D.N. Laikov, *Doklady Math.* 59 (1999) 477.
- [31] X.G. Wang, A Fortran code to generate Lebedev grids up to order L=131 is available at <<http://server.ccl.net/cca/software/SOURCES/>>, 2003.
- [32] G.M. Sheldrick, *SADABS* Program for Area Detector Absorption Correction, Institute for Inorganic Chemistry, University of Göttingen, Germany, 1996.
- [33] *SHELXTL 6.14* Version, Bruker AXS, Karlsruhe, Germany.
- [34] E.Y. Tshuva, I. Goldberg, M. Kol, *Organometallics* 20 (2001) 3017.
- [35] E.Y. Tshuva, S. Groysman, I. Goldberg, M. Kol, *Organometallics* 21 (2002) 662.
- [36] B. Akhlaghinia, E. Safaei, M. Asadi, submitted for publication.
- [37] E. Safaei, A. Wojtczak, E. Bill, H. Hamidi, *Polyhedron* 29 (2010) 2769.
- [38] H.L. Shyu, H.H. Wei, G.H. Lee, Y. Wang, *Inorg. Chem.* 35 (1996) 5396.
- [39] T. Kruse, T. Weyhermüller, K. Wieghardt, *Inorg. Chim. Acta* 331 (2002) 81.
- [40] M. Thirumavalavan, P. Akilan, M. Kandaswamy, K. Chinnakali, G.S. Kumar, H.K. Fun, *Inorg. Chem.* 42 (2003) 3308.
- [41] O. Kahn, *Molecular Magnetism*, ISBN 1-56081-566-3, VCH Publishers Inc., New York, 1993.
- [42] L.K. Thompson, S.K. Mandal, S.S. Tandon, J.N. Bridson, M.K. Park, *Inorg. Chem.* 35 (1996) 3117.
- [43] O. Kahn, *Inorg. Chim. Acta* 62 (1982) 3.
- [44] L. Merz, W. Haase, *J. Chem. Soc., Dalton Trans.* (1980) 875.
- [45] V.H. Crawford, H.W. Richardson, J.R. Wasson, D.J. Hodgson, W.C. Hatfield, *Inorg. Chem.* 15 (1976) 2107.
- [46] P.J. Hay, J.C. Thibeault, R. Hoffmann, *J. Am. Chem. Soc.* 97 (1975) 4884.